AIAA JOURNAL
Vol. 34, No. 1, January 1996

Effects of Shear and Strain on Temporal Evolution of Laminar Diffusion Flames

Nedunchezhian Swaminathan* and Shankar Mahalingam†
University of Colorado, Boulder, Colorado 80309-0427

Closed-form analytical solutions that describe the evolution of diffusion flames in two-dimensional laminar flowfields due to an initial line source of fuel in an infinite oxidizer environment are derived. The velocity field is assumed to be divergence free and both steady and unsteady shear and plane stagnation flows are considered in this study. The flame surface is modeled as an infinitesimally thin flame sheet at which fuel and oxidizer are consumed at an infinitely fast rate; thus, chemical kinetic effects are ignored. Validity of the solutions are discussed. The flame shapes are observed to be elliptic. The flame front moves away from the source at early times; whereas at later times, the front collapses at the location of the fuel source. An expression for the time for complete consumption of the fuel is derived in each case, and it is shown that strain fields are more conducive to combustion.

Nomenclature

A = aspect ratio of the elliptical front
a = shear rate
b = strain rate
C_f = mass concentration of fuel
$\mathcal{D}$ = mass diffusivity
e = base of natural logarithm
Pe = Peclet number identical to $L_{\text{ref}}^2/\mathcal{D}t_{\text{ref}}$
Q = mixture fraction source strength
$\hat{Q}$ = fuel source strength used in Eq. (1)
r_m = maximum radius of reaction front
t = nondimensional time
t_c = nondimensional time after which the solution is valid
t_e = nondimensional time for complete consumption of fuel
t_m = nondimensional time at which radius of reaction front is maximum
u = x component velocity
v = y component velocity
W_j = molecular weight of species j
x, y = nondimensional spatial coordinates
$\hat{x}, \hat{y}$ = dimensional spatial coordinates
Y_j = mass fraction of species j
$Y_{j,0}$ = mass fraction of species j at time $t = 0$
Z = mixture fraction
Z_c = stoichiometric mixture fraction
α = ratio of strain rate to its frequency of oscillation (a/ω)
β = Shvab–Zel'dovich variable
δ = Dirac delta function
ϵ = ratio of strain rate to its oscillation frequency (b/ω)
ν_i = stoichiometric moles of species i
ϕ = phase shift
ω = angular frequency

I. Introduction

DIFFUSION flames occurring in practical systems are inevitably unsteady and commonly turbulent in nature. Because of inherent complexities associated with turbulent combustion, mathematical analysis of these flames is difficult. To comprehend the behavior of turbulent flames, it is important to understand the fundamental characteristics of unsteady diffusion flames established in simplified situations. There are two parts to the fundamental attribute; one is related to flame structure and the other one is related to flame evolution. In this paper, we are interested in the flame evolution under various flow conditions. The simplified situations considered in this study are relevant to flame spread and turbulent flame modeling. A complete analysis must include a set of nonlinear partial differential equations including variable thermophysical properties and a chemical kinetic mechanism appropriate to the fuel-oxidizer combination. Including unsteady effects makes the problem all the more difficult. Since the interest in this paper is on unsteady effects, this aspect of the problem is retained, although several other aspects are simplified through appropriate assumptions. Virtually all analytical approaches to the problem, including this study, invoke thin flame approximation of Burke and Schumann.[1]

The study of diffusion flame spread is motivated by a need to control and prevent accidental fires that could occur in a wide variety of situations. Fernandez-Pello and Hirano[2] reviewed experimental and modeling work on diffusion flame spread with an emphasis on controlling mechanisms. De Ris[3] derived an expression for flame-spread velocity due to a diffusion flame spreading against an airstream over a fuel bed. Much of the past work has focused more on the spreading of flames over solid combustible substances than between gaseous fuels and oxidizers. However, controlled gaseous diffusion flames have received much attention since the celebrated analytical solution of Burke and Schumann.[1] Their predictions of shapes and heights of a steady coflowing laminar jet diffusion flame, under an infinitely fast chemistry assumption, compared well with experiments. Chung and Law[4] improved this solution by including streamwise diffusion. Williams[5] derived a form of the Burke–Schumann solution when the radius of the outer tube approaches infinity. Savas and Gollahalli[6] developed an exact solution to the concentration field of jet fluid in a laminar axisymmetric jet in the limit of zero heat release using Landau–Squires formulation.[7] Back diffusion of fuel behind its source was observed by Mahalingam[8] in his improved analysis of a self–similar diffusion flame solution obtained by Mahalingam et al.[9]

All of these analyses have been limited to steadily burning laminar diffusion flames. For unsteady cases, two of the more well-known solutions are due to Clarke and Stegen[10] and Bush and Fendell.[11] Using boundary-layer approximations, Clarke and Stegen[10] studied the effect of perturbations in reactant concentrations on the time-dependent response of a diffusion flame sheet established in a mixing layer environment. Bush and Fendell[11] examined the effects of a two-step finite rate reaction on time evolution of flames in unstrained one-dimensional and strained two-dimensional flows. They predicted that excessive strain could lead to departure from equilibrium resulting in a reduction in consumption rates. Since then, very little analytical work has appeared on unsteady laminar diffusion flames.

Under certain circumstances discussed in Sec. II, equations describing a laminar diffusion flame reduce to an equation governing a conserved scalar. This feature is exploited in this paper

Received Nov. 20, 1994; revision received March 20, 1995; accepted for publication March 23, 1995.

*Center for Combustion Research, Department of Mechanical Engineering. Student Member AIAA.
†Assistant Professor, Center for Combustion Research, Department of Mechanical Engineering. Member AIAA.

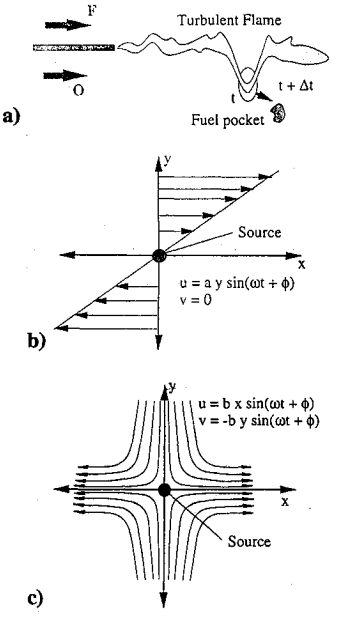

Fig. 1 Schematic representation of a) a turbulent diffusion flame and the flow configurations investigated, b) shear flow and c) plane strain field.

to develop a variety of time-dependent diffusion flame solutions. Several time-dependent solutions to diffusion of passive scalars in oscillating fluid flows exist in the literature.[12–17] Leighton[18] analyzed the diffusion of a point source of dilute solute in an oscillating shear flow and obtained a self-similar solution. Krishnan and Leighton[19] obtained self-similar solutions to diffusion of a passive scalar from a point source in plane and axisymmetric stagnation flows. In this paper, the solution approach of Leighton[18] and Krishnan and Leighton[19] is used to obtain solutions to diffusion flame shapes in simple linear two-dimensional flowfields. This allows us to predict flame front evolution and obtain expressions for time for complete consumption of a finite amount of fuel.

A typical turbulent flame in a mixing layer environment is shown in Fig. 1a. If the local gradients of velocity and scalar fields are appropriate, then the turbulent flame will extinguish locally.[20] This might allow a pocket of fuel (or oxidizer) to pass through the stoichiometric surface, as shown in Fig. 1a. This phenomenon has been observed recently by Higuera and Moser[21] in their simulation of turbulent reacting mixing layer. This pocket of fuel, wandering in oxidizer stream, might get ignited if the local conditions are appropriate and undergo an evolution process. Since the velocity at a position relative to a neighboring point can be decomposed into a symmetric and antisymmetric part, we considered a stagnant field, uniform flow, shear flows, strain, and rotational fields to study flame evolution.[22] Results for the stagnant, shear, and strain cases are presented in this paper.

In Sec. II, mathematical formulation of the problem including the significance of approximations introduced is described. Solution techniques are presented in Sec. III, followed by a discussion on the validity of solutions obtained. Results are discussed in Sec. V, and the important findings are summarized in Sec. VI.

II. Problem Formulation

The problem considered is a two-dimensional laminar diffusion flame established between fuel and oxidizer in an unbounded medium. Oxidizer is assumed to occupy the entire two-dimensional space. At time $t = 0$, a given mass (q^2) of fuel is introduced as an instantaneous (one-shot) line source located at the origin of the coordinate system as shown in Figs. 1b and 1c. This physical situation translates mathematically as an initial condition,

$$\int_{-\infty}^{\infty}\int_{-\infty}^{\infty} C_f(\hat{x},\hat{y},\hat{t}=0)\,\mathrm{d}x\,\mathrm{d}y = \int_{-\infty}^{\infty}\int_{-\infty}^{\infty} \tilde{Q}^2\delta(\hat{x})\delta(\hat{y})\,\mathrm{d}\hat{x}\,\mathrm{d}\hat{y} = q^2 \tag{1}$$

The flowfield is assumed to be divergence free so that the velocity field can be prescribed independent of chemical reaction process. The justification for this assumption is the ensuing problem can be treated analytically, relatively easily. In practice, this assumption may be reasonable in flows with sufficiently diluted fuel and oxidizer streams so that the adiabatic flame temperature is not significantly higher than the temperature of reactants. The reaction between fuel (F) and oxidizer (O) is assumed to occur in a single irreversible molar conserving global step to yield products of combustion (P) as

$$\nu_F F + \nu_O O \longrightarrow \nu_p P \tag{2}$$

The assumption of molar conservation is essential to ensure the validity of the divergence free velocity field at the locations of flame front. The reaction (2) is assumed to proceed at an infinitely fast rate leading to a reaction sheet. Liñán and Williams[23] indicate that this is a useful limit to consider because it can be uniformly valid in both space and time. In addition to the unity Lewis number assumption,[24] the diffusivities of all species are assumed to be constant and equal to each other. It is important to remark, however, that nonunity Lewis number effects are important in studies related to soot formation or flame extinction,[4] an aspect that is not considered in this paper.

Let $Y_{F,0}$ and $Y_{O,0}$ represent the fuel and oxidizer mass fractions in their unmixed state. Thus in general, the fuel (or oxidizer) introduced at the origin could be diluted with an inert species. Under the stated assumptions, we can define a conserved quantity $\beta \equiv Y_F/W_F\nu_F - Y_O/W_O\nu_O$. Since β decays asymptotically to $-Y_{O,0}/W_O\nu_O$, rather than to zero in the far field, it is convenient to define a mixture fraction[25] $Z \equiv [\beta - \beta_{O,0}]/[\beta_{F,0} - \beta_{O,0}]$, so that Z goes to zero in the far field (pure oxidizer) and $Z = 1$ in the pure fuel side. The reaction front is located at stoichiometric mixture fraction given by[5] $Z_c \equiv -\beta_{O,0}/[\beta_{F,0} - \beta_{O,0}]$.

The mixture fraction satisfies the following conserved scalar equation[5]:

$$\rho\frac{\partial Z}{\partial \hat{t}} + \rho\frac{\partial \hat{u}Z}{\partial \hat{x}} + \rho\frac{\partial \hat{v}Z}{\partial \hat{y}} = \rho D\left[\frac{\partial^2 Z}{\partial \hat{x}^2} + \frac{\partial^2 Z}{\partial \hat{y}^2}\right] \tag{3}$$

The initial condition for Eq. (3) corresponding to a line source of fuel at the origin, from Eq. (1), is given by $Z(\hat{x},\hat{y},\hat{t}=0) = Q^2\delta(\hat{x})\delta(\hat{y})$. This condition indicates that Z is unbounded, contradicting the fact that Z varies from zero to unity. Thus, it is important to emphasize that solutions obtained in this study are physically meaningful only after the fuel spreads out to a characteristic length scale as discussed in Sec. IV. The boundary condition for Eq. (3) is $Z(|\hat{x}|, |\hat{y}| \to \infty, t) \to 0$.

By integrating Eq. (3) over all space and noting that Z and ∇Z approach zero in the far field it can be shown[22] that the integral of Z is a conserved quantity. Thus,

$$\int_{-\infty}^{\infty}\int_{-\infty}^{\infty} Z(\hat{x},\hat{y},\hat{t})\,\mathrm{d}\hat{x}\,\mathrm{d}\hat{y} = Q^2 \tag{4}$$

This integral constraint suggests that Q may be used to construct a length scale in order to render Eq. (3) dimensionless. Using the symbol t_{ref} for a reference time scale one obtains

$$\frac{\partial Z}{\partial t} + u\frac{\partial Z}{\partial x} + v\frac{\partial Z}{\partial y} = \frac{1}{Pe}\left[\frac{\partial^2 Z}{\partial x^2} + \frac{\partial^2 Z}{\partial y^2}\right] \tag{5}$$

as the nondimensional form of Eq. (3) subject to initial and boundary conditions

$$Z(x,y,0) = \delta(x)\delta(y) \qquad \text{and} \qquad Z(|x|, |y| \to \infty, t) \to 0 \tag{6}$$

Self-similar shapes of the reaction front are obtained by setting $Z(x_f, y_f, t) = Z_c$ in solutions to Eq. (5). The time for complete consumption of the fuel is derived by setting $x_f = y_f = 0$.

III. Solution Method

Self-similar solutions to Eq. (5) subject to Eq. (6) are obtained following Leighton[18] and Krishnan and Leighton.[19] The details of solution process is very dependent on the specified flowfield.[18,19,22]

From the solutions derived for a variety of flowfields,[22] only stagnant, shear, and strain field cases are discussed in this paper. These flow situations are shown schematically in Figs. 1b and 1c.

A. Stagnant Field

This is a limiting case of other flowfields, where $u = v = 0$ in Eq. (5). Since the problem lacks a natural time scale, $Q^2/\mathcal{D}$ is chosen as t_{ref} leading to $Pe = 1$. Solution to this case can be readily written as $Z = (4\pi t)^{-1} \exp[-r^2/4t]$, where $r^2 = x^2 + y^2$. The characteristics of this solution are discussed and compared with earlier experimental and theoretical results in Sec. V.A.

B. Shear Flows

The dimensional velocity components for the steady and unsteady cases are given as $u = ay$, $v = 0$ and $u = ay \sin(\omega t + \phi)$, $v = 0$ respectively. In the steady case, choosing t_{ref} as $1/a$ and substituting the assumed form of u and v into Eq. (5) yields

$$\frac{\partial Z}{\partial t} + y\frac{\partial Z}{\partial x} = \frac{1}{Pe}\left[\frac{\partial^2 Z}{\partial x^2} + \frac{\partial^2 Z}{\partial y^2}\right] \tag{7}$$

subject to Eq. (6). Since diffusion is the only process occurring in the y direction, a separable solution in the form[18] $Z(x, y, t) = f(x, y, t)g(y, t)$ is sought. After some algebraic manipulations an unsteady diffusion equation for g, subject to $g(|y| \to \infty, t) \to 0$ and $g(y, 0) = \delta(y)$, the following equation for f is obtained:

$$f_t + yf_x = [f_{xx} + f_{yy} + 2f_y g_y/g]/Pe \tag{8}$$

Note that subscripts denote appropriate partial derivatives. The initial and boundary conditions for Eq. (8) are $f(x, y, 0) = \delta(x)$ and $f(|x|, |y| \to \infty, t) \to 0$. The g equation has the solution

$$g(y, t) = \sqrt{Pe/(4\pi t)} \exp[-y^2 Pe/4t] \tag{9}$$

Substituting this result into Eq. (8) and defining $\tau = t, \eta = x - y\tau/2$, and $\xi(\tau) = \tau + \tau^3/12$, a diffusion equation[18,22] in ξ and η can be obtained for f, after equating the coefficient of convective term to zero in order to get a self-similar solution. Combining the solutions of g and f we obtain

$$Z(x, y, t) = \frac{Pe}{4\pi\sqrt{t\xi}} \exp\left[-\frac{Pe}{4}\left(\frac{\eta^2}{\xi} + \frac{y^2}{t}\right)\right] \tag{10}$$

In unsteady shear case, choosing $1/\omega$ as reference time scale and following the above described procedure, we obtain Eq. (10) as a solution with[18,22] $\eta = x - \alpha y h(t)$, where

$$h(t) = \cos\phi\left(\frac{\sin t}{t} - \cos t\right) + \sin\phi\left(\frac{\cos t - 1}{t} + \sin t\right) \tag{11}$$

$$\xi(t) = t + \alpha^2(0.5[t + \sin(t + \phi)\cos(t + \phi)] - [\sin(t + \phi) - \sin\phi]^2/t) \tag{12}$$

C. Strain Fields

For steady and unsteady strain fields, the dimensional velocity components are prescribed as $u = bx$, $v = -by$, and $u = bx \sin(\omega t + \phi)$, $v = -by \sin(\omega t + \phi)$, respectively. In the unsteady case we have a choice of either $1/b$ or $1/\omega$ as a reference time scale. Using $t_{ref} = 1/\omega$ and substituting the dimensionless velocity components in Eq. (5), we obtain

$$\frac{\partial Z}{\partial t} + \epsilon \sin(t + \phi)\left(x\frac{\partial Z}{\partial x} - y\frac{\partial Z}{\partial y}\right) = \frac{1}{Pe}\left(\frac{\partial^2 Z}{\partial x^2} + \frac{\partial^2 Z}{\partial y^2}\right) \tag{13}$$

The initial and boundary conditions are given by Eq. (6). Following Krishnan and Leighton[19] a solution of the form $Z(x, y, t) = f(x, t)\, g(y, t)$ is sought. Similar to the procedure for shear flows, a solution for Z is obtained as

$$Z(x, y, t) = \frac{Pe}{4\pi\sqrt{\xi_1\xi_2}} \exp\left[-\frac{Pe}{4}\left(\frac{\eta_1^2}{\xi_1} + \frac{\eta_2^2}{\xi_2}\right)\right] \tag{14}$$

where

$$\tau = t, \qquad \eta_1 = xh_1(\tau)$$
$$h_1(\tau) = \exp[\epsilon(\cos(\tau + \phi) - \cos\phi)] \tag{15}$$

$$\eta_2 = yh_2(\tau), \qquad h_2(\tau) = \exp[-\epsilon(\cos(\tau + \phi) - \cos\phi)] \tag{16}$$

$$\xi_1 = \int_0^\tau h_1^2(\tau')\, d\tau' \qquad \xi_2 = \int_0^\tau h_2^2(\tau')\, d\tau' \tag{17}$$

In the case of a steady strain field, it can be shown[22] that Eq. (14) forms the solution with $\eta_1 = xe^{-t}$, $\eta_2 = ye^t$, $\xi_1 = (1 - e^{-2t})/2$, and $\xi_2 = (e^{2t} - 1)/2$ by choosing $1/b$ as t_{ref}.

IV. Solution Validity

Since Z is mixture fraction, it varies from zero to unity. But the initial condition, Eq. (6), indicates that Z is unbounded. Hence, the solutions are physically valid only when the mixture fraction value lies between zero and one. This occurs after some elapsed time t_c. This t_c can be obtained by setting $Z(0, 0, t_c) = 1$ in the mixture fraction field solutions. Perhaps, there may be other choices for t_c. In steady cases, we can obtain a closed-form solution to t_c, whereas in unsteady situations t_c is obtained by solving appropriate transcendental equations numerically.

V. Discussion

A. Stagnant Field

A limiting situation is the case where the flame spreads in a stagnant field. Solution to this problem is given in Sec. III.A. This solution is valid only after $t_c = 1/4\pi$. From symmetry, one expects the flame front to be circular. Denoting the radius of the stoichiometric surface by $r_f = \sqrt{(x_f^2 + y_f^2)}$, we obtain $r_f(t) = 2\sqrt{(t\ell_n[1/(4\pi Z_c t)])}$.

Several interesting observations may be made. The flame radius reaches a maximum $r_m = (\pi e Z_c)^{0.5}$ at time $t_m = (4\pi e Z_c)^{-1}$. Thus, the solution predicts that the flame spreads rapidly from the source at earlier times. During this process, combustion products spread away from reaction zone, thereby diluting the reactants (fuel and oxidizer) on either side of the front. Consequently, the reactant flux, being proportional to reactant concentration gradient, reduces. This retards the rate of flame spread until the flame radius reaches r_m at time t_m. Subsequently, the stoichiometric burning condition can be maintained only if r_f decreases. The fuel is completely consumed in time $t_e = et_m$. A plot of flame radius as a function of time for two different values of Z_c is shown in Fig. 2. Because of the singular behavior of the solution at early times, the physically valid region ($t_c \geq 1/4\pi$) is also marked in Fig. 2. The Z_c values chosen are representative of methane burning in air ($Z_c = 0.05507$) and oxygen ($Z_c = 0.2$).

This limiting case is identical to Spalding's solution[26] of a point source of fuel vapor in a supercritical oxidizer environment. He found that the commonly invoked quasisteady assumption in studies of droplet combustion failed when the droplet was introduced

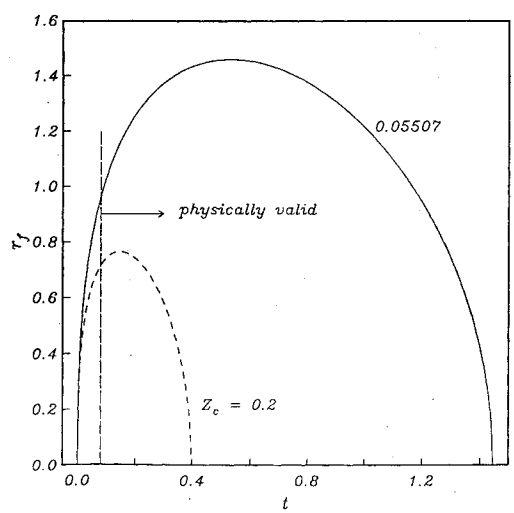

Fig. 2 Variation of flame radius with time in a stagnant field.

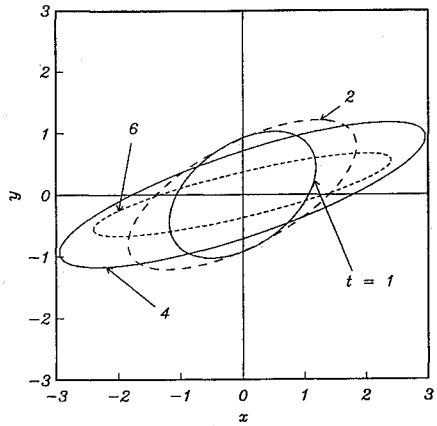

Fig. 3 Contours of reaction front at different times in a steady shear flow for $Pe = 10, Z_c = 0.05507$.

in a near-critical or supercritical oxidizer environment. He, thus, modeled the droplet as an instantaneous point source of fuel vapor and included the unsteady term in the governing equation. The differences in the exact form of his and our solution stems from the fact that he considered a three-dimensional point source, whereas we are examining a two-dimensional line source. The consistency, however, of the temporal evolution, existence of a maximum flame radius, consumption of fuel in a finite time, etc., with Spalding's solution and experimental observations of burning droplets even at atmospheric (subcritical) conditions,[27] validates our solution.

In summary, both t_m and t_e vary inversely with Z_c whereas the maximum flame radius r_m is inversely proportional to its square root as shown in Fig. 2. Note, however, that the dimensional maximum flame radius is proportional to source strength Q whereas the corresponding dimensional time is proportional to the square of the source strength and is inversely related to diffusion coefficient. In Spalding's solution,[26] r_m varies as $Q^{1/3}$ and $Z_c^{-1/3}$ whereas t_e varies as $Q^{2/3}$ and $Z_c^{-2/3}$, indicating a higher burning rate in a three-dimensional case.

B. Shear Flow

Let us first consider the steady case in which the shear rate is fixed in time. The locus of the reaction front obtained from Eq. (10) is an ellipse given by

$$\frac{(x_f - y_f t/2)^2}{(1 + t^2/12)} + y_f^2 = \frac{4t}{Pe} \ell_n \left[\frac{Pe}{4\pi Z_c t \sqrt{1 + t^2/12}} \right] \tag{18}$$

This is plotted in Fig. 3 after $t_c = [\sqrt{(36 + 3(Pe/2\pi)^2)} - 6]^{1/2}$. At early times, the reaction front spreads out equally along both coordinate directions [see Eq. (19)]. As the front spreads out in the y direction, however, it finds itself in regions of significant shear. This results in the front locus becoming elliptical with its axes rotated in the shear direction as shown in Fig. 3.

The orientation of the principal axes of the ellipse, measured in counterclockwise direction, is given by $\vartheta = 0.5[\tan^{-1}(3/t)]$. It is apparent that $\vartheta \to \pi/4$ as $t \to 0$ and $\vartheta \to 0$ as $t \to \infty$. The first limit is independent of shear rate as long as the magnitude of the shear rate is bounded, whereas the second limit depends on the magnitude. Since diffusion enhances convection along x, the major axis of the elliptic front is much larger than its minor axis at all times.[22] The aspect ratio of the ellipse $\mathcal{A}$, defined as the ratio of major to minor axes lengths,

$$\mathcal{A}^2(t) = \frac{\sqrt{9 + t^2}(6 + t^2) + t^3 + 9t}{\sqrt{9 + t^2}(6 + t^2) - t^3 - 9t} \tag{19}$$

indicates that $\mathcal{A} \to 1$ as $t \to 0$, whereas, $\mathcal{A}(t_e) \neq 1$. Thus, the topology of the reactive-diffusive front is very dependent on its history. Fuel depletion results in the reaction front ultimately shrinking toward the origin as indicated in Fig. 3 with the fuel completely consumed in a time $t_e = [\sqrt{(36 + 3(Pe/2\pi Z_c)^2)} - 6]^{1/2}$.

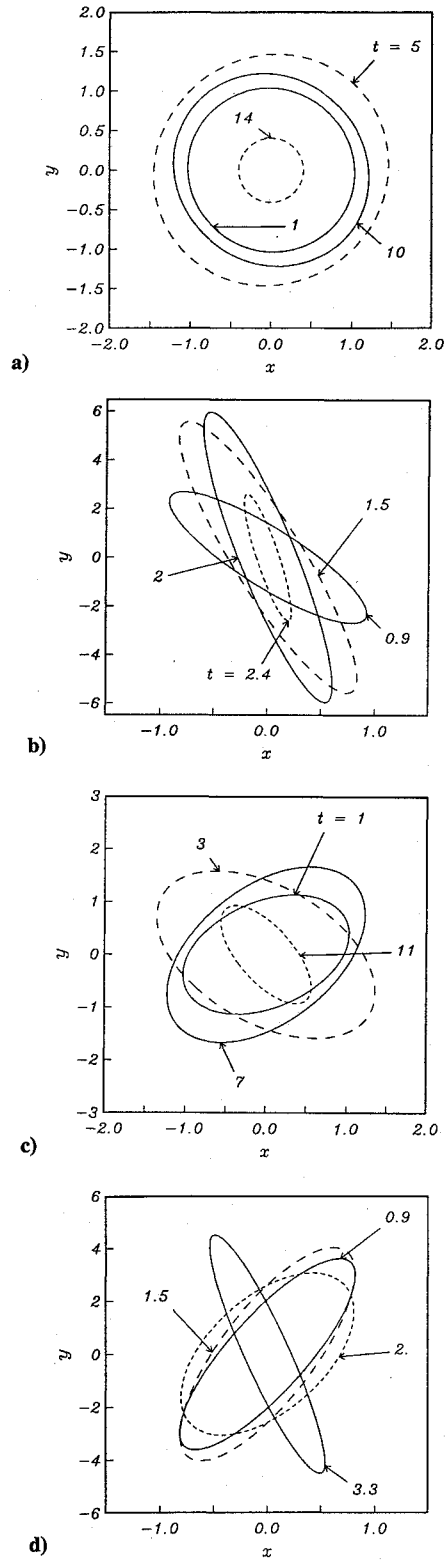

Fig. 4 Temporal evolution of flame topology in unsteady shear flows for $Pe = 10, Z_c = 0.05507$ with a) $\alpha = 0.1, \phi = 0$; b) $\alpha = 10.0, \phi = 0$; c) $\alpha = 1.0, \phi = -\pi/2$; and d) $\alpha = 10.0, \phi = -\pi/2$.

Shapes of reaction front in an oscillating shear flow given by

$$\frac{[x_f - \alpha y_f h(t)]^2}{\xi(t)} + \frac{y_f^2}{t} = \frac{4}{Pe} \ell_n \left[\frac{Pe}{4\pi Z_c \sqrt{t\xi(t)}} \right] \tag{20}$$

are shown in Fig. 4. Expressions for $h(t)$ and $\xi(t)$ are given by Eqs. (11) and (12). Reaction fronts plotted after t_c in Fig. 4 are elliptic with their axes rotating periodically with time. The flame spreads by diffusion in the y direction, while it spreads along x due to both convective and diffusive effects as in steady case, and

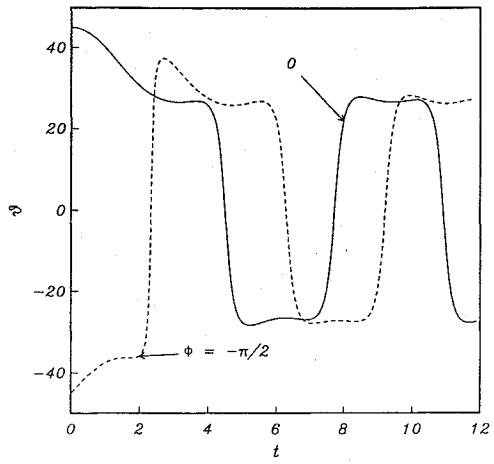

Fig. 5 Evolution of tilt angle ϑ of ellipse in an unsteady shear flow for $\alpha = 1$, $Pe = 10$, and $Z_c = 0.05507$.

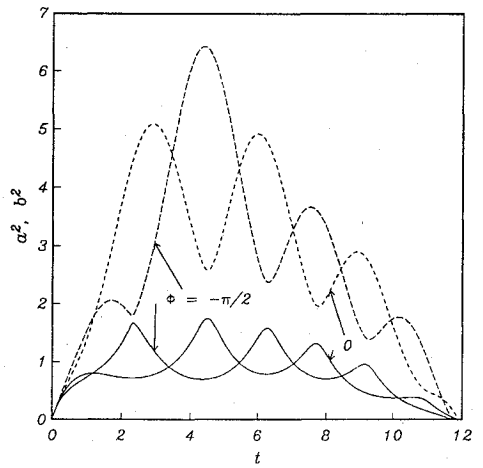

Fig. 6 Evolution of the square of semimajor (dotted lines) and semiminor (solid lines) axes in an unsteady shear flow for $\alpha = 1$, $Pe = 10$, and $Z_c = 0.05507$.

additionally the shear tends to rotate the reaction front. The reaction front spreads away from the origin as a circle at early times. This outward spread is curtailed because of fuel depletion. Thus, at later times, the ellipses shrink in size until all of the fuel is consumed. Larger values of α, corresponding to a stronger shear, results in a rapid stretching of the front along with a rapid tilt as shown in Figs. 4b and 4d. Under weak shear conditions the flame evolves as if it were in a stagnant field, as indicated by Fig. 4a. The orientation of the principal axes of these elliptical fronts is given by

$$\vartheta = 0.5 \tan^{-1}\left[\frac{-2\alpha h t}{t - \xi - \alpha^2 h^2 t}\right] \tag{21}$$

As $t \to 0$, $\vartheta \to \pi/4$, indicating that the reaction front evolves with its major axis oriented at 45 deg irrespective of shear strength and initial phase shift.[22] The temporal evolution of ϑ is shown in Fig. 5 for a typical case. The dramatic reduction in ϑ corresponds to a slight change in the topology when the axes of the ellipse shift quadrants. This apparent singularity is physically admissible and can undergo several cycles depending on α and ϕ. The variation of square of semimajor and minor axes of the elliptical front shown in Fig. 6 also indicates the presence of this singularity. For smaller values of the ratio of oscillatory time scale to flow time scale ($\alpha = 0.1$) the amplitude of the oscillation of ϑ is 45 deg whereas for $\alpha = 10$, ϑ varies between -10 and 10 deg (Ref. 22).

The time for complete consumption t_e varies linearly with Peclet number. Higher value of α results in shorter consumption times. The effect of ϕ on t_e is negligible in cases with stronger source having either stronger shear rate or a rapidly oscillating shear. For smaller value of Z_c, the effect of ϕ on t_e is negligible irrespective of source strength, shear rate, and oscillation frequency.[22]

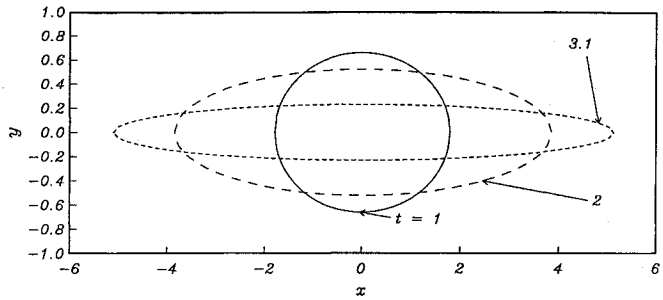

Fig. 7 Temporal evolution of the flame topology in a steady strain field for $Pe = 10$ and $Z_c = 0.05507$.

C. Plane Strain Fields

Solution for the steady and oscillating strain field is given by Eq. (14) with proper definition of η and ξ given in Sec. III.C. In the case of the steady strain field, the flame locus is given by

$$\frac{x_f^2}{\exp(2t) - 1} + \frac{y_f^2}{1 - \exp(-2t)} = \frac{2}{Pe} \ell n\left(\frac{Pe}{2\pi Z_c \sqrt{2(\cosh 2t - 1)}}\right) \tag{22}$$

The flame fronts plotted after time $t_c = 0.5 \cosh^{-1}[1 + Pe^2/8\pi^2]$ are shown in Fig. 7. At early times the front spreads out in a near circular fashion. Convection enhances diffusion along x whereas the opposite is the case along y. The result is that the initially near-circular-shaped reaction front is distorted into an elliptical shape with major and minor axes aligned with strain directions. An interesting point to be observed in Fig. 7 is that the minor axis length does not exceed the characteristic length scale unlike in oscillating strain cases, whereas the major axis length reaches a value of about an order higher than the characteristic length scale. This is due to a strong convective effect along x. At later times the flame spreads out along x while it shifts inward toward the origin along y due to fuel depletion until the front collapses on the x axis. The fuel is completely consumed in a finite time t_e given by $0.5 \cosh^{-1}(1 + Pe^2/8\pi^2 Z_c^2)$.

An expression for the locus of the stoichiometric surface in an oscillating strain field is given by

$$Z_c = \frac{Pe}{4\pi\sqrt{\xi_1 \xi_2}} \exp\left[-\frac{Pe}{4}\left(\frac{\eta_{1f}^2}{\xi_1} + \frac{\eta_{2f}^2}{\xi_2}\right)\right] \tag{23}$$

where η_1, η_2, ξ_1, and ξ_2 are defined by Eqs. (15–17). The reaction fronts shown in Fig. 8 are elliptic as in the steady strain case. In the unsteady case the critical time t_c is obtained by solving an implicit equation $\xi_1(t_c)\xi_2(t_c) - Pe^2/16\pi^2 = 0$. The topological behavior of the reaction front is very dependent on the parameters ϵ and ϕ. Higher values of ϵ correspond to a slowly oscillating strain field with a high strain rate. Since the strain rate is high, the reaction fronts are stretched rapidly in the strain direction, as indicated in Fig. 8b. Figures 8b and 8d are given to indicate the effect of ϕ. The time lag between fluid dynamic and chemical processes is related to the initial phase shift. In stronger strain rate cases, when ϕ is nonzero, the fuel is consumed at a faster rate so that complete fuel consumption is realized before the reaction front becomes highly elliptic. This fact is eludicated in Fig. 8d (see also Fig. 9b). Depending on the value of ϵ, the aspect ratio of the elliptic front is either monotonously increasing or oscillating for $\phi = 0$, whereas for $\phi = -\pi/2$, the aspect ratio is nearly unity throughout the evolution. If the ratio of oscillatory time scale to that of strain rate is of order unity, however, axes switching can occur depending on the initial phase.[22] For low values of ϵ, this axis switching can undergo several cycles until complete fuel consumption is realized in time t_e. The time t_e is given by an implicit equation

$$\int_0^{t_e} \exp[2\epsilon \cos(\tau + \phi)]\, d\tau \int_0^{t_e} \exp[-2\epsilon \cos(\tau + \phi)]\, d\tau = \frac{Pe^2}{16\pi^2 Z_c^2} \tag{24}$$

For low values of $\epsilon (= 0.1)$, we can see that t_e varies linearly with Pe as shown in Fig. 9a by taking a limit $\epsilon \to 0$ in Eq. (24). For

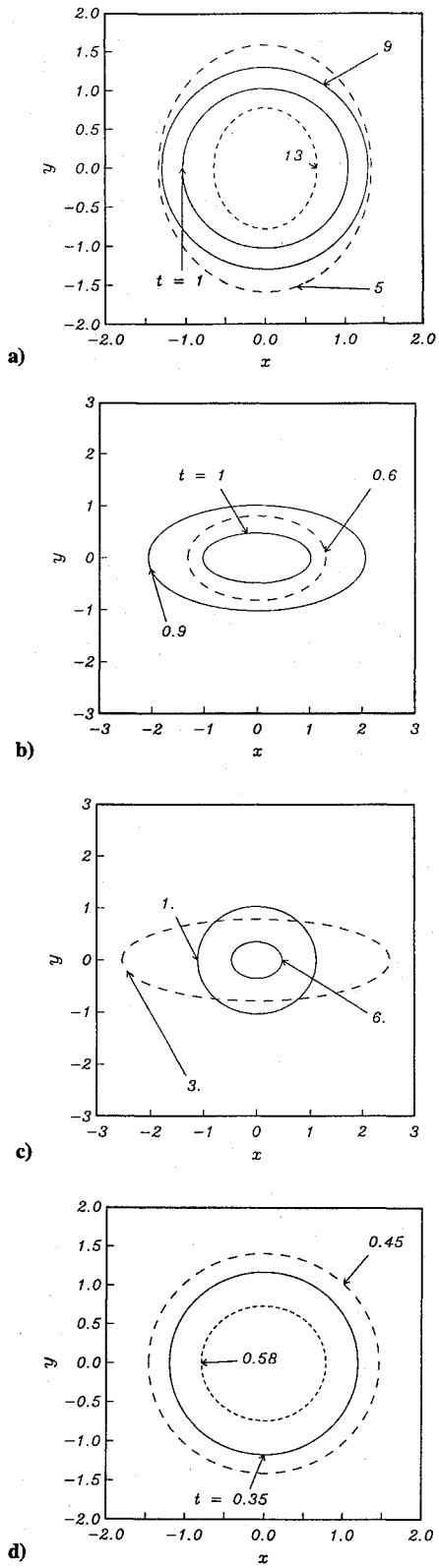

Fig. 8 Temporal evolution of flame topology in oscillating strain fields for $Pe = 10, Z_c = 0.05507$ with a) $\epsilon = 0.1, \phi = 0$; b) $\epsilon = 10.0, \phi = 0$; c) $\epsilon = 1.0, \phi = -\pi/2$; and d) $\epsilon = 10.0, \phi = -\pi/2$.

moderate values of ϵ, t_e oscillates over a linear variation as shown in Fig. 9a. The effect of the initial phase was found to be negligible for these cases. For higher values of ϵ, however, ϕ has stronger effects on t_e as shown in Fig. 9b. This may perhaps be due to history effects. Figure 9b also indicates that in cases with stronger strain rate, t_e dependence on Pe becomes weaker for a stronger source, unlike in cases with stronger shear rates. This observation suggests that the strain fields are more conducive to combustion.

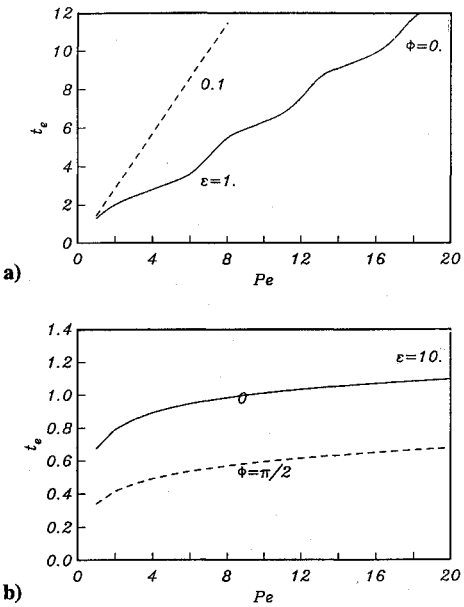

Fig. 9 Variation of t_e with Pe in an oscillating strain field for $Z_c = 0.05507$.

VI. Summary and Concluding Remarks

The evolution of two-dimensional laminar diffusion flames due to a line source of fuel in an infinite oxidizer medium have been examined for a stagnant field, steady and unsteady shear, and strain fields. All of these flowfields are characterized by the fact that velocity components are linearly related to distance from the fuel source. Under stagnant flow conditions, flame contours are circular. The flame spreads out to a maximum radius and then collapses back toward the origin in a finite time. In the presence of a uniform shear flow, the contours are continuously stretched by convection in the direction of the local velocity; the resulting reaction fronts are elliptical and whereas the mean shear flow oscillates sinusoidally with time, the axes of these fronts rotate periodically. When the flame evolves in a steady plane strain field, the initially near-circular-shaped flame is stretched in the direction along which convection and diffusion aid each other. Correspondingly, the spread of the flame in the orthogonal direction is retarded, leading to an elliptic flame shape with its axes aligned with the strain directions. At later times, the flame front shrinks inward until all of the fuel is completely consumed. When the strain field is allowed to oscillate sinusoidally in time, axes switching can occur depending on the initial phase and ϵ. In all cases studied, we can predict the time for complete consumption as a function of problem parameters. This time varies linearly with source strength in all shear cases and in cases with low to moderate strain rate, whereas under high-strain rates t_e has a weaker dependence, for a stronger source, indicating that t_e becomes almost independent of source strength. This means that the strain fields are more conducive to the combustion process.

Based on the present results, it is relatively straightforward to write down solutions for the case of a point source of fuel for various flow configurations studied by recognizing that diffusion in the z direction is uninfluenced by the flowfield. Results for three-dimensional flame topology may be readily obtained by multiplying the present solutions to Z by a one-dimensional diffusion equation solution along z. Although the solutions derived are for sinusoidally oscillating flows, it is possible to handle other types of time-dependent flows that may be appropriate in open fire-spread situations. These solutions can be extended to account for distributed fuel sources in order to model more realistic configurations. Furthermore, it is possible to obtain species mass fraction and temperature profiles a posteriori from the solution to the mixture fraction presented in this paper using standard methods as outlined by Williams.[5] However, experimental verification of the predictions discussed in this paper are required before one examines these cases. Note that partial theoretical and experimental support

for the simplest case of stagnant flow provides confidence on the validity of other solutions presented in this paper.

Acknowledgments

The authors acknowledge partial support from the University of Colorado at Boulder for the research presented in this paper. In addition, acknowledgment is made to the Donors of The Petroleum Research Fund, administered by the American Chemical Society, for partial support of this research through a Type G Grant. The first author acknowledges useful discussions with Patrick D. Weidman and Harvey Segur.

References

[1]Burke, S. P., and Schumann, T. E. W., "Diffusion Flames," *Industrial Engineering Chemistry*, Vol. 20, 1928, pp. 998–1004.

[2]Fernandez-Pello, A. C., and Hirano, T., "Controlling Mechanisms of Flame Spread," *Combustion Science and Technology*, Vol. 32, No. 1, 1983, pp. 1–31.

[3]de Ris, J. N., "Spread of a Laminar Diffusion Flame," *Proceedings of Twelfth Symposium (International) on Combustion*, Combustion Inst., Pittsburgh, PA, 1969, pp. 241–252.

[4]Chung, S. H., and Law, C. K., "Burke–Schumann Flame with Streamwise and Preferential Diffusion," *Combustion Science and Technology*, Vol. 37, No. 1, 1984, pp. 21–46.

[5]Williams, F. A., *Combustion Theory*, 2nd ed., Addison–Wesley, Menlo Park, CA, 1985, pp. 73–75.

[6]Savas, Ö., and Gollahalli, S. R., "Stability of Lifted Laminar Round Gas–jet Flame," *Journal of Fluid Mechanics*, Vol. 165, April 1986, pp. 297–318.

[7]Batchelor, G. K., *An Introduction to Fluid Dynamics*, Cambridge Univ. Press, Cambridge, England, UK, 1967, pp. 205–211.

[8]Mahalingam, S., "Self-similar Diffusion Flame Including Effects of Streamwise Diffusion," *Combustion Science and Technology*, Vol. 89, No. 5, 1993, pp. 363–373.

[9]Mahalingam, S., Ferziger, J. H., and Cantwell, B. J., "Self-similar Diffusion Flame," *Combustion and Flame*, Vol. 82, 1990, pp. 231–234.

[10]Clarke, J. F., and Stegen, G. R., "Some Unsteady Motions of a Diffusion Flame Sheet," *Journal of Fluid Mechanics*, Vol. 34, Nov. 1968, pp. 343–358.

[11]Bush, W. B., and Fendell, F. E., "Diffusion-flame Structure for a Two-step Chain Reaction," *Journal of Fluid Mechanics*, Vol. 64, July 1974, pp. 701–724.

[12]Tennekes, H., and Lumley, J. L., *A First Course in Turbulence*, MIT Press, Cambridge, MA, 1972, pp. 230–241.

[13]Foister, R. T., and van de Ven, T. G. M., "Diffusion of Brownian Particles in Shear Flows," *Journal of Fluid Mechanics*, Vol. 96, Jan. 1980, pp. 105–132.

[14]Watson, E. J., "Diffusion in Oscillatory Pipe Flow," *Journal of Fluid Mechanics*, Vol. 133, Aug. 1983, pp. 233–244.

[15]Aris, R., "On the Dispersion of a Solute in Pulsating Flow Through a Tube," *Proceedings of the Royal Society A*, Vol. 259, 1960, pp. 370–376.

[16]Taylor, G., "Dispersion of Soluble Matter in Solvent Flowing Slowly Through a Tube," *Proceedings of the Royal Society of London, Series A: Mathematical and Physical Sciences*, Vol. 219, 1954, pp. 186–203.

[17]Eckmann, D. M., and Grotberg, J. B., "Oscillatory Flow and Mass Transport in a Curved Tube," *Journal of Fluid Mechanics*, Vol. 188, March 1988, pp. 509–527.

[18]Leighton, D. T., "Diffusion From an Initial Point Distribution in an Unbounded Oscillating Simple Shear Flow," *Physico Chemical Hydrodynamics*, Vol. 11, 1989, pp. 377–386.

[19]Krishnan, G. P., and Leighton, D. T., "Diffusion From a Point Source in a Time-dependent Unbounded Extensional Flow," *Physics of Fluids A*, Vol. 4, Nov. 1992, pp. 2327–2331.

[20]Lockwood, F. C., and Megahed, I. E. A., "Extinction in Turbulent Reacting Flows," *Combustion Science and Technology*, Vol. 19, No. 1, 1978, pp. 77–80.

[21]Higuera, F. J., and Moser, R. D., "Effect of Chemical Heat Release in a Temporally Evolving Mixing Layer," *CTR Summer Proceedings*, 1994, pp. 19–40.

[22]Swaminathan, N., "Structure and Dynamics of Turbulent and Laminar Reaction Zones," Ph.D. Thesis, Univ. of Colorado, Boulder, CO, 1994.

[23]Liñán, A., and Williams, F. A., "Fundamental Aspects of Combustion," *Oxford Engineering Science Series 34*, Oxford Univ. Press, New York, 1993, pp. 63, 64.

[24]Law, C. K., "Heat and Mass Transfer in Combustion: Fundamental Concepts and Analytical Techniques," *Progress in Energy Combustion Sciences*, Vol. 10, 1984, pp. 295–318.

[25]Libby, P. A., and Williams, F. A., "Fundamental Aspects," *Turbulent Reacting Flows*, edited by P. A. Libby and F. A. Williams, Vol. 44, Springer–Verlag, Berlin, 1980, pp. 66, 67.

[26]Spalding, D. B., "Theory of Particle Combustion at High Pressures," *Journal of the American Rocket Society*, Vol. 29, 1959, pp. 828–835.

[27]Okajima, S., and Kumagai, S., "Further Investigations of Combustion of Free Droplets in a Freely Falling Chamber Including Moving Droplets," *Proceedings of Fifteenth Symposium (International) on Combustion*, Combustion Inst., Pittsburgh, PA, 1975, pp. 401–407.